

Aberrant Gene Expression Profiles in Pluripotent Stem Cells Induced from Fibroblasts of a Klinefelter Syndrome Patient*

Received for publication, May 10, 2012, and in revised form, September 19, 2012 Published, JBC Papers in Press, September 27, 2012, DOI 10.1074/jbc.M112.380204

Yu Ma^{‡§}, Chunliang Li^{‡§1}, Junjie Gu^{‡§}, Fan Tang^{‡§}, Chun Li^{‡§}, Peng Li[¶], Ping Ping[¶], Shi Yang[¶], Zheng Li^{¶2}, and Ying Jin^{‡§3}

From the [‡]Key Laboratory of Stem Cell Biology, Institute of Health Sciences, Shanghai Jiao Tong University School of Medicine and Shanghai Institutes of Biological Sciences, Chinese Academy of Sciences, the [§]Shanghai Stem Cell Institute, Shanghai Jiao Tong University School of Medicine, 225 South Chongqing Road, Shanghai, 200025, and the [¶]Department of Urology, Sperm Development and Genetics Laboratory, Shanghai Human Sperm Bank, Shanghai Institute of Andrology, Renji Hospital, Shanghai Jiao Tong University School of Medicine, 145 Shandong Zhong Road, Shanghai 200001, China

Background: Pathophysiology for Klinefelter syndrome (KS) is poorly explained due to the lack of adequate models.

Results: KS-iPSCs exhibit aberrantly expressed genes associated with the clinical features of KS.

Conclusion: KS-iPSCs can potentially serve as a cellular model for KS research.

Significance: Our study will significantly accelerate the understanding, diagnosis, and treatment of Klinefelter syndrome.

Klinefelter syndrome (KS) is the most common male chromosome aneuploidy. Its pathophysiology is largely unexplained due to the lack of adequate models. Here, we report the derivation of induced pluripotent stem cell (iPSCs) lines from a KS patient with a karyotype of 47, XXY. Derived KS-iPSCs meet all criteria of normal iPSCs with the potential for germ cell differentiation. Although X chromosome inactivation occurs in all KS-iPSCs, genome-wide transcriptome analysis identifies aberrantly expressed genes associated with the clinical features of KS. Our KS-iPSCs can serve as a cellular model for KS research. Identified genes may become biomarkers for early diagnosis or potential therapeutic targets for KS and significantly accelerate the understanding, diagnosis, and treatment of Klinefelter syndrome.

Klinefelter syndrome (KS)⁴ is the most common genetic form of male hypogonadism due to a supernumerary X chromosome, with an estimated frequency between 1/1000 and 1/500 (1). About 90% of KS patients bear the 47, XXY karyotype, whereas the 46, XX/47, XXY mosaic karyotype and, less frequently, additional X chromosomes (48, XXXY, and 49,

XXXY) are found in the remaining KS patients (2). Clinically, KS is generally characterized by a reduced testicular volume, azoospermia, and some other features such as tall stature, gynecomastia, increased serum FSH excretion, and androgen deficiency, although its clinical picture exhibits a broader spectrum of phenotypes (2). Moreover, compared with normal males, KS patients have a higher risk to suffer from many other disorders, such as osteoporosis, metabolic syndrome, diabetes, breast cancer, and subtle cognitive deficits (3–6). There is currently no effective treatment for KS. Intracytoplasmic sperm injection with spermatozoa obtained by testicular sperm extraction techniques would give some KS males a chance to father a child, whereas for most of the patients, infertility is still unresolved due to the failure of sperm retrievals or spermatogenesis (1, 2). Therefore, further understanding of the disease and developing new strategies are required for effective treatment of KS.

Despite extensive studies in the past decades, the link of supernumerary X chromosomes to KS phenotypes and molecular mechanisms underlying the testicular degeneration remain a mystery due to the lack of adequate and convenient experimental models. The advent of induced pluripotent stem cells (iPSCs) by defined transcriptional factors, particularly those derived from patients, provides a new and attractive alternative for the *in vitro* disease model (7, 8). Similar to embryonic stem cells (ESCs), iPSCs have characteristics of unlimited self-renewal and pluripotent developmental potential. Disease-specific iPSCs would not only provide a renewable cell source but also recapitulate the disease in a Petri dish to model the development of the disease *in vitro* (9). Until now, iPSCs derived from somatic cells of various diseases have been applied in disease models and have presented the unique opportunity to develop novel disease treatment strategies that have thus far not been possible (10).

In this study, we generated four lines of iPSCs from foreskin fibroblast cells of a KS patient with the 47, XXY karyotype and explored their potential usage for modeling the development of KS disease *in vitro*. The results obtained here will facilitate our

* This work was supported by National High Technology Research and Development Program of China Grants 2010CB945200, 2011DFB300100, 2011CB965101, and 2009CB941103, National Natural Science Foundation Grant 91019023, Chinese Academy of Science Grant XDA01010102, Shanghai Leading Academic Discipline Project Grant S30201, and Key Project of Shanghai Municipal Education Commission Grant 10ZZ70.

¹ Present address: Dept. of Tumor Cell Biology, Howard Hughes Medical Institute/St. Jude Children's Research Hospital, 262 Danny Thomas Place MS 350, Ste. D5017, Memphis, TN 38105.

² To whom correspondence may be addressed: 145 Shandong Zhong Rd., Shanghai, 200001, China. Tel.: 86-21-6373-2926; E-mail: doc.zheng.li@gmail.com; Lizhengboshi@163.com.

³ To whom correspondence may be addressed: Bldg. 1, Rm. 607, 225 South Chongqing Rd., Shanghai 200025, China. Tel.: 86-21-6385-2591; Fax: 86-21-6385-2591; E-mail: yjin@sibs.ac.cn.

⁴ The abbreviations used are: KS, Klinefelter syndrome; DEG, differentially expressed gene; EB, embryoid body; ESC, embryonic stem cell; hESC, human ESC; fs, fibroblast; G, Giemsa; iPSC, induced pluripotent stem cell; N, normal; XCI, X chromosome inactivation; BMP, bone morphogenetic protein.

This is an Open Access article under the CC BY license.

understanding of this particular disease and identify potential new targets for its treatment.

EXPERIMENTAL PROCEDURES

Derivation and Culture of Primary Fibroblast Cells from the Foreskin—Discarded foreskins of a normal subject and a Klinefelter syndrome patient were obtained from the Renji Hospital with the approval of the Reproductive Ethical Committee of the hospital after getting the written informed consents from the donors. The procedures of the derivation and culture of the fibroblast cells were same as described previously (11).

iPSC Derivation and Culture—For iPSC derivation, the virus was prepared as described previously (12, 13). About 10^5 fibroblast cells were cultured in the medium with four viruses containing supernatant and Polybrene overnight. About 24 h later, the fibroblast cells were digested into single cells and replated onto gelatin-coated dishes. Culture medium was replaced by the iPSC culture medium the next day. The iPSC culture medium was the KO-DMEM with 20% knock-out serum replacement (Invitrogen), 100 units/ml penicillin, 100 μ g/ml streptomycin, 0.1 mM β -mercaptoethanol (Sigma), 2 mM L-glutamine, 1% nonessential amino acid (Invitrogen), and 4 ng/ml bFGF (R&D Systems). iPSC colonies were passaged by collagenase IV (5 mg/ml, Invitrogen) or the mechanical method every 5 days.

Alkaline Phosphatase Staining—iPSC colonies were fixed with 4% paraformaldehyde in PBS and permeabilized by 0.1% Triton X-100 in PBS. The colonies were treated with alkaline phosphatase staining solution as instructed by the alkaline phosphatase substrate kit III manual (Vector Laboratories, Inc.) for 30–45 min in 37 °C.

G Banding Analysis—Cells were cultured with 100 ng/ml colchicine (Sigma) for 12–16 h. Then the cells were digested by 0.25% trypsin/EDTA (Invitrogen) into single cells, treated by hypotonic solution, including 0.16 g of potassium chloride and 0.125 g of sodium citrate in 50 ml of deionized water, for 30 min, and fixed by glacial acetic acid and methyl alcohol at a 1:3 ratio for 30 min. Then samples were analyzed at the Da An Co. (Shanghai, China).

Immunofluorescence Staining—Cells were plated on glass slides and fixed with 4% paraformaldehyde in PBS. Immunofluorescence staining was performed as reported previously (12). The information regarding the primary antibodies is shown in Table 1.

RT-PCR and Quantitative RT-PCR—Total RNA of cells was extracted by TRIzol (Invitrogen) and reverse-transcribed into cDNA using ReverTra Ace reverse transcriptase and oligo(dT)₁₅. PCRs were carried out in the systems reported previously (14). For quantitative PCR, manufacturer's instructions (ABI PRISM 7900) were followed. For detection of the expression levels of germ cell lineage markers, GAPDH and RPLPO were used as internal controls, and averages of the ΔC_t values were calculated for analysis. For other detections, only GAPDH was used as an internal control. The sequences of primers for RT-PCR, pMXs-OCT4, pMXs-SOX2, pMXs-KLF4, pMXs-C-MYC and RPLPO have been reported previously (12, 15–18). Sequences of primers used to amplify *MAGEA2B*, *MAGEH1*,

TABLE 1
Information of antibodies

Protein	Company
Vimentin	Abcam
OCT4	Prepared by our laboratory
SOX2	Prepared by our laboratory
NANOG	R&D Systems
SSEA4	Millipore
TRA-1–60	Millipore
TRA-1–81	Chemicon
AFP	DAKO
SOX17	R&D Systems
FLK1	Santa Cruz Biotechnology
NESTIN	Millipore
TUJ1	Promega
VASA	Abcam
H3K27me3	Millipore
macroH2A1	Active Motif

TABLE 2
Information on primers

Gene	Sequences
For quantitative PCR	
NANOG	F, GAATGAAATCTAAGAGGTGGCA R, CCTGGTGGTAGGAAGAGTAAAGG
VASA	F, TCGGATAACCATTAGCACAG R, ATCATCTACTGGATTGGGAGC
STRA8	F, CAACCCAGAAAACCCAGAGGAGA R, CTTTCATCAACGGGAAAGGATGCT
BLIMP1	F, ACGGCCTTTCAAATGTCAGACTTG R, TCTTGAGATTGCTGGTGTGCTAA
IFITM1	F, TCACTCAACACTTCCTTCCCAAAA R, TCGCCAACCATCTCTGTGTCCTA
PELO	F, AGTGAAGACCCGACAACTGCT R, CTCACCTGCTTGAGTCCATAGAA
GAPDH	F, TCCACCCATGGCAAATTC R, TCGCCCCACTTGATTTTGG
XIST	F, GGCACCTAGCACTTGAGGAT R, GAGAAACATGGAAATGGGTAA
ZXDA	F, TTCACCACCTCTTACAAGCTCA R, CTCACATTGAACGAGTTCTCCT
For BSP	
OCT4 (outside)	F, GTTAAGGTTAGTGGGTGGGATT R, ATCACCTCCACCACCTAAAAA
OCT4 (inside)	F, AGAGAGGGGTTGAGTAGTTTTTT R, ACCTCCACCACCTAAAAAAAC

NRK, and *TMEM47* were from PrimerBank. Sequences of other primers are shown in Table 2.

Bisulfite Sequencing PCR—Two μ g of genomic DNA was treated according to the procedures of Active Motif. Nested PCR was carried out with primers provided in Table 2. PCR products were purified and ligated to the pGEM-T easy vector (Promega) for sequencing.

DNA FISH Assay—Cells were digested into single cells with 0.25% trypsin/EDTA and suspended in PBS. Then the cells were treated with hypotonic solution with 0.16 g of potassium chloride and 0.125 g of sodium citrate in 50 ml of deionized water and fixed by solution with glacial acetic acid and methanol in a 1:3 volume ratio. Cell nuclei were collected, and DNA FISH assays were performed by Da An Co. (Shanghai, China).

EB Formation—iPSCs were cultured on low attachment dishes with the human EB medium containing KO-DMEM, 20% fetal bovine serum (Hyclone), 100 units/ml penicillin, 100 μ g/ml streptomycin, 0.1 mM β -mercaptoethanol, 2 mM L-glutamine, 1% nonessential amino acid for 9 days. Then EBs were collected and replated onto Matrigel-coated glass covers for additional 2 days.

Teratoma Formation—About 5×10^6 iPSCs were cultured in the presence of 10 μ M Y27632 (Calbiochem) overnight,

iPSC Lines of a Klinefelter Syndrome Patient

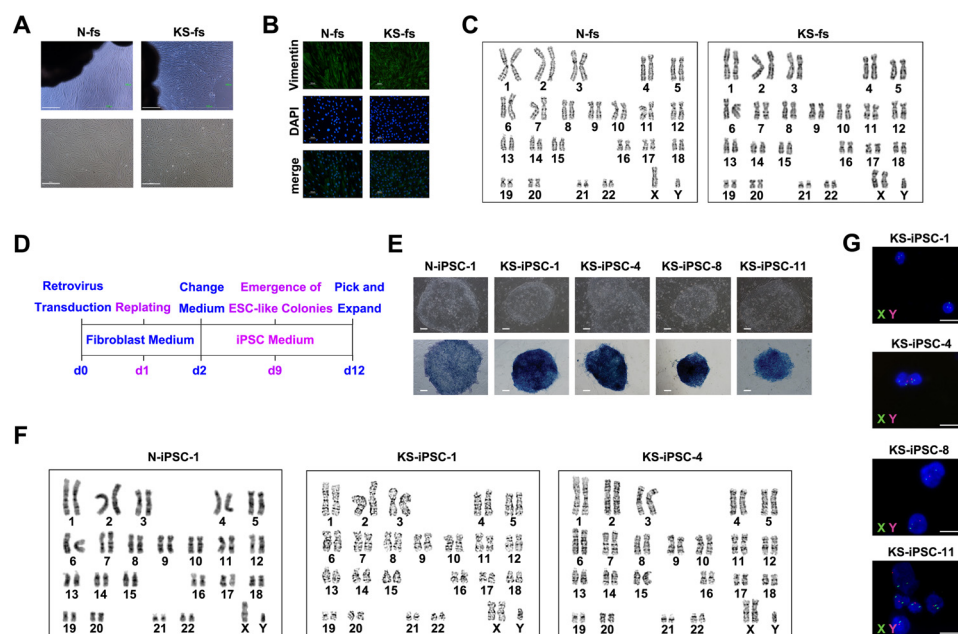


FIGURE 1. Generation of iPSC lines from fibroblast cells (fs) of a normal subject and a KS patient. A, primary culture of N-fs and KS-fs. Upper panel shows fs migrating from foreskin tissue clumps. Bottom panel shows the morphology of fs. Scale bars, 100 μ m. B, immunofluorescence staining of N-fs and KS-fs with an antibody against Vimentin. Scale bars, 50 μ m. C, G banding karyotypes of N-fs and KS-fs. N-fs have a normal 46, XY karyotype, and KS-fs display an abnormal 47, XXY karyotype. D, flow diagram of the iPSC induction. E, morphology and alkaline phosphatase staining of cells from N-iPSC-1 and KS-iPSC-1, -4, -8, and -11. Scale bars, 100 μ m. F, G banding analysis of cells from N-iPSC-1 and KS-iPSC-1 and -4. G, DNA FISH assays identify the two X chromosomes and a Y chromosome in cells of KS-iPSC-1, -4, -8, and -11. Scale bars, 25 μ m.

and then collected and injected intramuscularly into SCID mice. About 2 months later, teratomas were collected for H&E staining.

Microarray Analysis—For each kind of cells, three biological repeats of samples were prepared. All experiments were performed with Affymetrix U133 plus 2.0 gene chips at Shanghai Biotechnology Corp. Raw data were normalized by MAS 5.0 algorithm, and DEGs were analyzed by Gene Spring Software 11.0 (Agilent Technologies, Santa Clara, CA). Scatter plots comparing the global gene expression profiles were constructed by the R software. Differentially expressed genes with a fold change of 1.5 were analyzed in the context of Gene Ontology and Kyoto Encyclopedia of Genes and Genomes (KEGG) pathway using DAVID 6.7 (david.abcc.ncifcrf.gov). The microarray data from this publication have been submitted to GEO database (ncbi.nlm.nih.gov) with an accession number of GSE37258.

Germ Cell Lineage Differentiation—For spontaneous differentiation, iPSCs at 5×10^4 were plated to 6-well plates and cultured in iPSC medium without bFGF. For BMP induction, iPSCs at 5×10^4 were plated to 6-well plates and cultured in the human EB medium supplemented with 10 μ M of BMP4, BMP7, and BMP8a (R&D Systems). For both methods, the medium was replaced every 7 days. Samples on the 7th, 14th, or 21st day were collected for gene expression analysis.

VASA Immunofluorescence Staining—Cells were digested by 0.25% trypsin/EDTA into single cells and plated on glass slides by cytospin at $200 \times g$ for 3 min. The prepared samples were fixed with 4% paraformaldehyde in PBS for immunofluorescence staining.

Statistical Analysis—All values except as otherwise indicated were analyzed by Student's *t* test to determine the significance

of the differences. *p* value < 0.05 was considered statistically significant.

RESULTS

Derivation of iPSC Lines from Foreskin Fibroblast Cells of a KS Patient and a Normal Subject—We established fibroblast cell lines from the foreskin tissue of a normal male and a KS patient, designating them as normal fibroblasts (N-fs) and KS fibroblasts (KS-fs), respectively (Fig. 1, A and B). The KS patient is 27 years old with typical KS symptoms such as hypogonadism and small size of testes in the clinical diagnosis. G banding examination indicated the karyotype of 46, XY for N-fs and 47, XXY for KS-fs (Fig. 1C). All of the cells of KS-fs carried the 47, XXY karyotype, implying that the KS foreskin donor might belong to the group of the most common KS cases with a homogeneous 47, XXY karyotype.

Reprogramming of both types of fibroblasts was induced by transduction of retroviral OCT4, SOX2, KLF4, and c-MYC as shown in Fig. 1D. The human embryonic stem cell (hESC)-like colonies were picked on day 12 of infection and expanded to establish the stable iPSC lines. In total, we established one normal iPSC line (N-iPSC-1) and four KS iPSC lines (KS-iPSC-1, -4, -8, and -11). There was no discernible difference in terms of reprogramming speed and efficiency between N-fs and KS-fs. iPSCs from both N-fs and KS-fs exhibited a typical morphology of hESCs and had the same karyotypes as their cognate fibroblasts, suggesting the maintenance of initial karyotypes throughout the reprogramming process (Fig. 1, E and F). The XXY karyotype of KS-iPSCs was further verified by fluorescence *in situ* hybridization assays (Fig. 1G). In addition, the pattern of seven short tandem repeat sites further verified the origin of N-iPSCs and KS-iPSCs (Table 3).

TABLE 3

STR detection of normal and KS iPSCs

	C5FIPO	D5S818	D7S820	D13S317	D16S539	TH01	TPOX
SHhES2	305.31	147.5	204.75	173.36	154.58	156.05	231.61
SHhES2	309.4	155.86	217.24	189.68	162.71	168.11	239.82
N-fs	^a	147.39	221.4	173.57	150.71	168.13	231.52
N-fs	309.71	151.81	*	181.63	158.84	171.23	243.8
N-iPSC-1	*	147.48	221.33	173.45	150.71	168.17	231.65
N-iPSC-1	313.48	151.81	*	181.59	158.84	171.22	243.87
KS-fs	305.4	151.82	212.93	185.55	146.23	155.96	231.56
KS-fs	313.64	155.91	217.08	189.65	154.77	168.01	243.91
KS-iPSC-1	305.51	150.8	212.88	186.03	146.01	155.86	231.47
KS-iPSC-1	313.68	154.93	217.02	190.01	154.58	167.88	243.75
KS-iPSC-4	305.32	150.81	213.03	185.55	146.09	156.11	231.5
KS-iPSC-4	313.51	154.93	217.15	189.56	154.68	168.2	244.41
KS-iPSC-8	305.36	151.81	212.93	185.77	146.51	155.91	231.51
KS-iPSC-8	313.48	155.95	217.05	189.84	155.07	167.94	243.76
KS-iPSC-11	305.37	150.81	212.93	185.45	146.3	155.96	231.48
KS-iPSC-11	313.53	154.98	217.08	189.55	154.82	167.97	243.75

^a * means undetected.

Characterization of iPSC Lines—To characterize iPSC lines described above, we first determined the expression of pluripotency-associated markers in comparison with hESCs of the SHhES2 line, which carried a normal 46, XY karyotype and was fully characterized previously (15). Cells of all established iPSC lines were alkaline phosphatase-positive (Fig. 1E), and endogenous expression of *NANOG*, *REX1*, *FGF4*, *LEFTY*, and *TDGF-1* as well as *OCT4*, *SOX2*, *KLF4*, and *c-MYC* was activated (Fig. 2A). Immunofluorescence staining assays also demonstrated the expression of OCT4, SOX2, NANOG, SSEA4, TRA-1–60 and TRA-1–81 in iPSCs (Fig. 2B). Simultaneously, the expression of transgenic genes in iPSCs was silenced significantly (Fig. 2C). Furthermore, similar to hESCs, the *OCT4* promoter was hypomethylated in all iPSCs, whereas it was hypermethylated in the starting fibroblasts, further verifying the reprogramming of fibroblasts (Fig. 2D).

Next, we assessed the developmental potential of our iPSCs through both *in vitro* and *in vivo* assays. EBs formed when iPSCs were cultured in suspension. Various types of cells grew out of EBs after attachment. Immunofluorescence staining revealed the presence of cells expressing endoderm (SOX17 and AFP), mesoderm (Vimentin and FLK1) and ectoderm (NESTIN and TUJ1) markers (Fig. 2E). In addition, teratomas, which contained the respiratory epithelium and goblet cells (endoderm), muscles and cartilage (mesoderm), and neural rosettes and pigmented cells (ectoderm), were detected 4–8 weeks after iPSCs were injected into immune-deficient mice (Fig. 2F).

To further define the iPSCs at a global transcriptional level, we compared the transcriptomic feature by scatter plots. As a result, all iPSCs tested approximated to hESCs (correlation coefficient >0.97) but not to their cognate fibroblasts (correlation coefficient <0.65) (Fig. 2G). Therefore, N-fs and KS-fs were successfully reprogrammed into the pluripotent state at a genome-wide transcriptional level.

X Chromosome Inactivation in KS-iPSCs—In female cells with a 46, XX karyotype, one of two X chromosomes is inactivated to balance the expression dosage of X chromosome-linked genes with 46, XY male cells. X chromosome inactivation (XCI) is one of the epigenetic regulations in mammalian cells and is initiated by coating of noncoding *XIST* RNA on X chromosomes followed by exclusion of active chromatin mark-

ers and subsequent accumulation of repressive markers, such as H3K27me3 and macroH2A1 (19). It has been shown that the mosaic pattern of XCI in normal female fibroblasts was converted to be clonal in human iPSCs after reprogramming (20). The question of whether XCI occurs in KS-iPSCs has not been addressed. We began by examining *XIST* expression levels in different types of fibroblasts and found that the level of *XIST* in KS-fs was similar to that in normal female fibroblasts (F-fs) but was significantly higher than that in male normal fibroblasts (N-fs) and hESCs (SHhES2) (Fig. 3A). Moreover, we found an extraordinarily high mRNA level of *XIST* in KS-iPSCs (Fig. 3B). These observations suggested the undergoing of XCI in both normal female and KS cells. Furthermore, inactive X chromosome (Xi)-like accumulations of H3K27me3 and macroH2A1 were detected in almost all of the KS-iPSCs, whereas only part of KS-fs displayed this enrichment pattern (Fig. 3, C and D). This phenomenon of differential XCI patterns detected between KS-fs and KS-iPSCs was similar to that observed between normal female fibroblasts (data not shown) and normal female iPSCs (F-iPSC), a previously reported iPSC line derived from human amniotic fluid-derived cells (hAFDC-iPSC-4) (12). As a negative control, the staining for H3K27me3 and macroH2A1 was not found in normal male fibroblasts (N-fs) (Fig. 3, C and D). Thus, one of the X chromosomes in our KS-iPSCs was inactive as in normal female cells.

Aberrant Transcriptome of KS-iPSCs—Although we detected the Xi-like accumulation of repressive markers in all KS-iPSCs, which differentiated into various cell types of the three germ layers in a manner similar to N-iPSCs, there might be aberrant gene expression in KS-iPSCs. First, XCI escaping has been demonstrated in females as well as in KS patients, implying that cells from KS patients may have two active copies of strictly X-linked genes (21). Second, KS-iPSCs could have three active copies of X-Y homologous genes from pseudoautosomal regions (22). To address this issue, global gene expression profiles of KS-iPSCs (KS-iPSC-1 and -4) were compared with those of normal control cells (N-iPSC-1 and SHhES2). A total of 105 genes was identified as differentially expressed genes (DEGs) with more than a 1.5-fold difference ($p < 0.05$). Among them, 76 genes had higher expression levels, and 29 genes had lower expression levels in KS-iPSCs than in control cells. The pathway analysis in the DAVID (Database for Annotation Visualization and Inte-

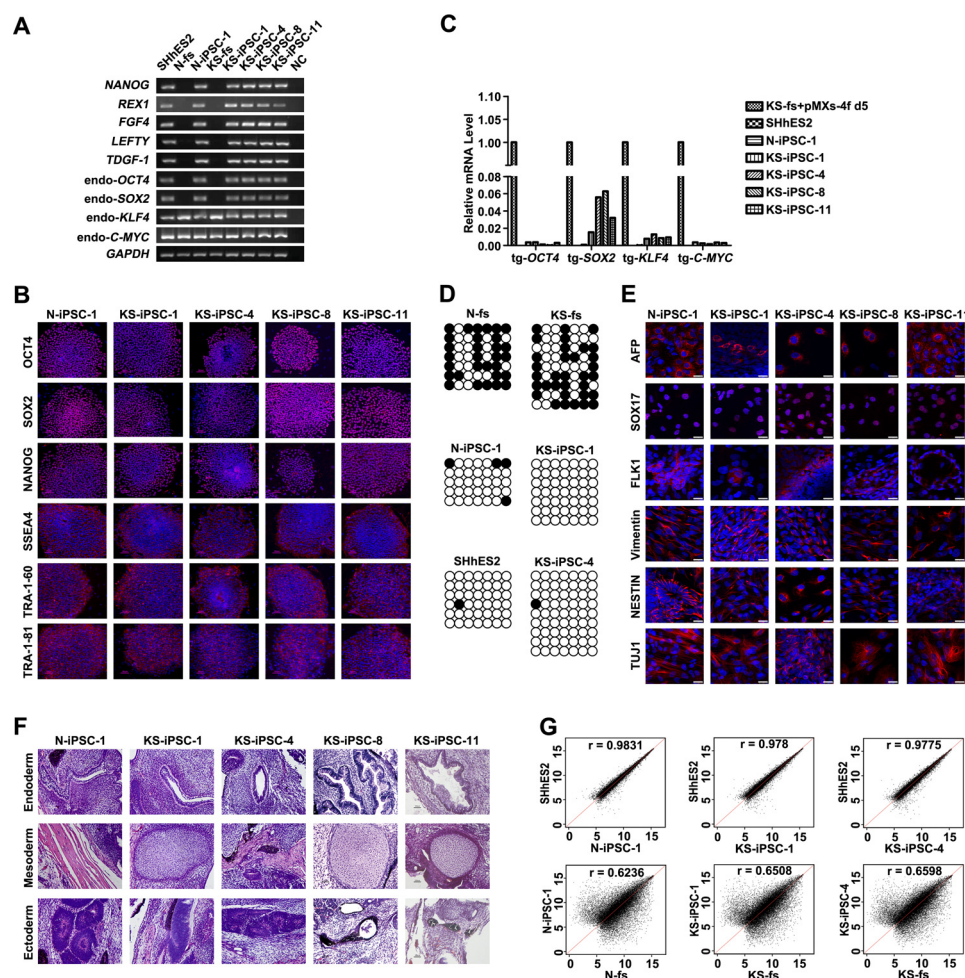


FIGURE 2. Characterization of iPSCs from N- and KS-fs. *A*, RT-PCR assays for the expression of pluripotency-associated markers in N-iPSC-1 and KS-iPSC-1, -4, -8, and -11. *B*, immunofluorescence staining using antibodies against OCT4, SOX2, NANOG, SSEA4, TRA-1-60, and TRA-1-81 in iPSCs of N-iPSC-1 and KS-iPSC-1, -4, -8, and -11. *C*, quantitative RT-PCR analysis of expression levels of four transgenic factors in N-iPSC-1 and KS-iPSC-1, -4, -8, and -11. The expression level of each gene in KS fibroblasts transfected with retroviruses containing sequences of transgenic *OCT4*, *SOX2*, *KLF4*, and *c-MYC* for 5 days was set as 1. The values were from one experiment. *D*, bisulfite sequencing analysis of endogenous *OCT4* promoter methylation in N-fs, KS-fs, N-iPSC-1, KS-iPSC-1 and -4, and SHHES2. *Open circles* denote unmethylated CpG sites, and *black circles* denote methylated CpG sites. *E*, immunofluorescence staining of differentiated cells from the EBs formed by N-iPSC-1 and KS-iPSC-1, -4, -8, and -11 using antibodies against AFP, SOX17 (endoderm), FLK1, Vimentin (mesoderm), NESTIN, and TUJ1 (ectoderm). *Scale bars*, 25 μ m. *F*, H&E staining of teratoma sections from N-iPSC-1, KS-iPSC-1, -4, -8, and -11. Respiratory epithelium and goblet cells (endoderm), muscles and cartilage (mesoderm), neural epithelium, and pigment cells (ectoderm) are shown. *Scale bars*, 50 μ m. *G*, global gene expression profiles of N-iPSC-1 and KS-iPSC-1 and -4 were compared with those of SHHES2, N-fs, and KS-fs by scatter plots analysis; *r* stands for correlation efficient.

grated Discovery) system indicated the enrichment of the DEGs in some diseases, especially in autoimmune diseases (Fig. 4A), which might reflect an increased risk for KS patients to suffer from autoimmune diseases such as systemic lupus erythematosus (23). Additionally, progesterone-mediated oocyte maturation was one of the enriched pathways (Fig. 4A), which could be linked to the female-like features of KS patients. Moreover, genes associated with the protein catabolic process were also differentially expressed (Fig. 4B). In fact, the metabolic syndrome is one of important clinical features of KS (1). Gene Ontology analysis also revealed distinct properties of the KS-iPSCs. For instance, DEGs encoded molecules with properties of being intrinsic to plasma membrane parts of the cells. The enriched biological processes included the immune regulation, protein catabolic process, and response to DNA damage stimulus (Fig. 4B). The aberrant expression of genes associated with these biological processes might correspond to the abnormalities of early embryo development in KS patients and cause com-

plicated disease phenotypes during later development of embryos or post puberty.

We also analyzed the DEGs between KS-iPSCs and normal controls based on a 2-fold difference criterion and focused on the X-linked genes. A total of 39 DEGs were identified. Twenty nine of them had higher levels, and the other 10 genes had lower levels in KS-iPSCs as compared with the control group (Fig. 4C). Intriguingly, 10 out of 29 genes having higher levels but none of genes with lower levels in KS-iPSCs were located on X chromosomes (Fig. 4, D and E), in line with the overdosage of X chromosomes in KS cells. The quantitative RT-PCR analysis further verified higher expression levels of X-linked genes, such as *XIST*, *MAGEA2B*, *MAGEH1*, *NRK*, *TMEM47*, and *ZXDA*, in KS-iPSCs (Figs. 3B and 4F). These genes have been known to participate in the pathways or biological processes that were enriched by the DEGs between KS-iPSCs and normal controls. For instance, *MAGEH1* belongs to the type II MAGE gene family and plays important roles in cell survival, cell cycle progres-

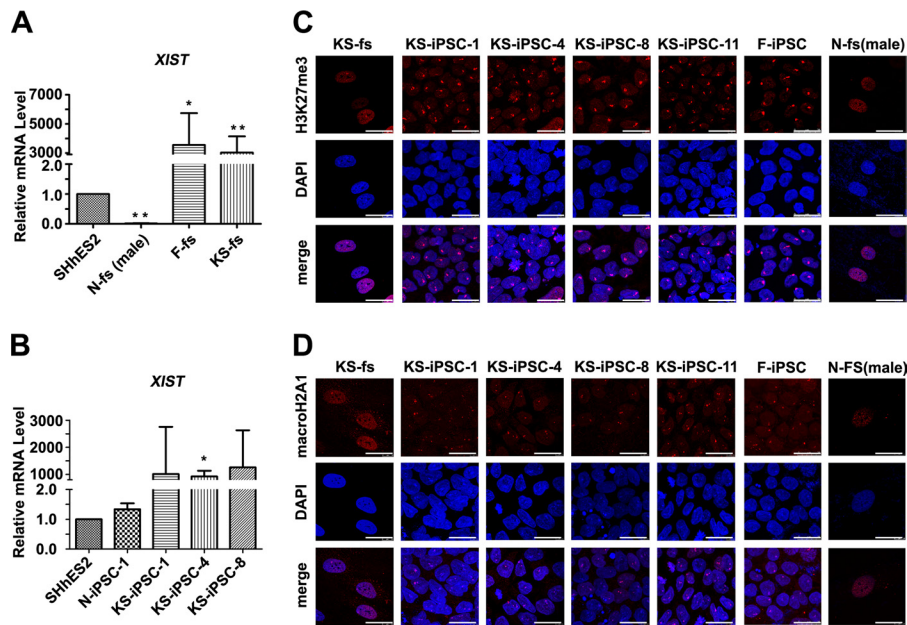


FIGURE 3. **Detection of X chromosome inactivation in KS-iPSCs.** A and B, quantitative RT-PCR analysis of the expression level of *XIST*. F-fs stands for normal female fibroblasts cultured from the human skin. Error bars, S.D.; *, $p < 0.05$; **, $p < 0.01$, $n = 3$. The expression level of genes in SHhES2 was set as 1. C, immunofluorescence staining of H3K27me3 in KS-fs, KS-iPSC-1, -4, -8, and -11, F-iPSC, and N-fs. The F-iPSC is a line of female iPSCs generated from human amniotic fluid-derived cells. N-fs stands for normal male fibroblasts. Scale bars, 25 μ m. D, immunofluorescence staining of macroH2A1 in KS-fs, KS-iPSC-1, -4, -8, and -11, F-iPSC, and N-fs. Scale bars, 25 μ m.

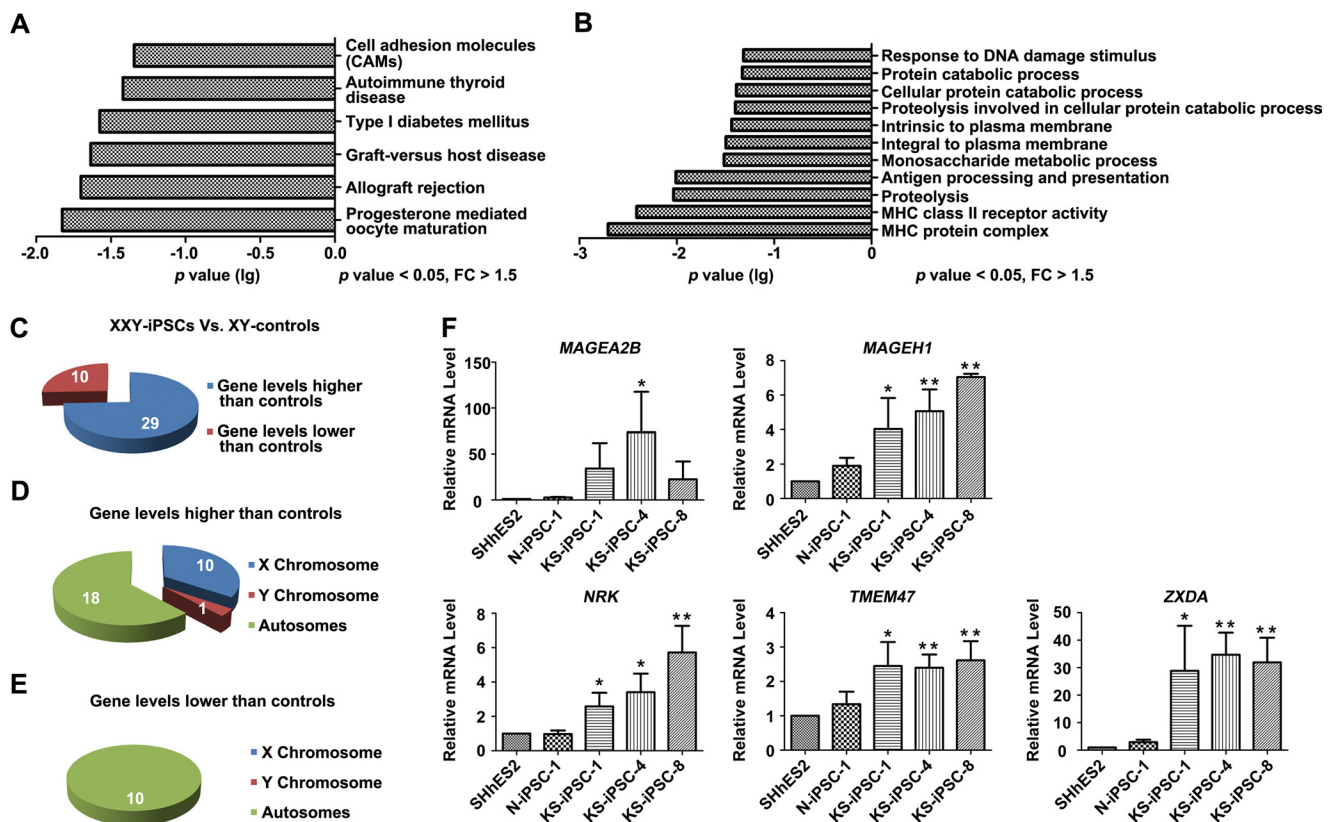


FIGURE 4. **Transcriptome analysis of DEGs between KS-iPSCs and normal controls.** A, KEGG pathway analysis of DEGs in KS-iPSC-1 and -4) compared with those in controls (N-iPSC-1 and SHhES2). Fold change (FC) > 1.5, p value < 0.05. B, Gene Ontology analysis of DEGs in KS-iPSCs compared with those in controls. Fold change > 1.5, p value < 0.05. C, D, and E, DEGs in KS-iPSCs with 47, XXY compared with normal 46, XY controls. Fold change > 2, p value < 0.05. The number of DEGs is shown in the figure. F, quantitative RT-PCR analysis of X-linked dysregulated genes (fold change > 2). Error bars, S.D.; *, $p < 0.05$; **, $p < 0.01$, $n = 3$. The expression levels of genes in SHhES2 were set as 1.

iPSC Lines of a Klinefelter Syndrome Patient

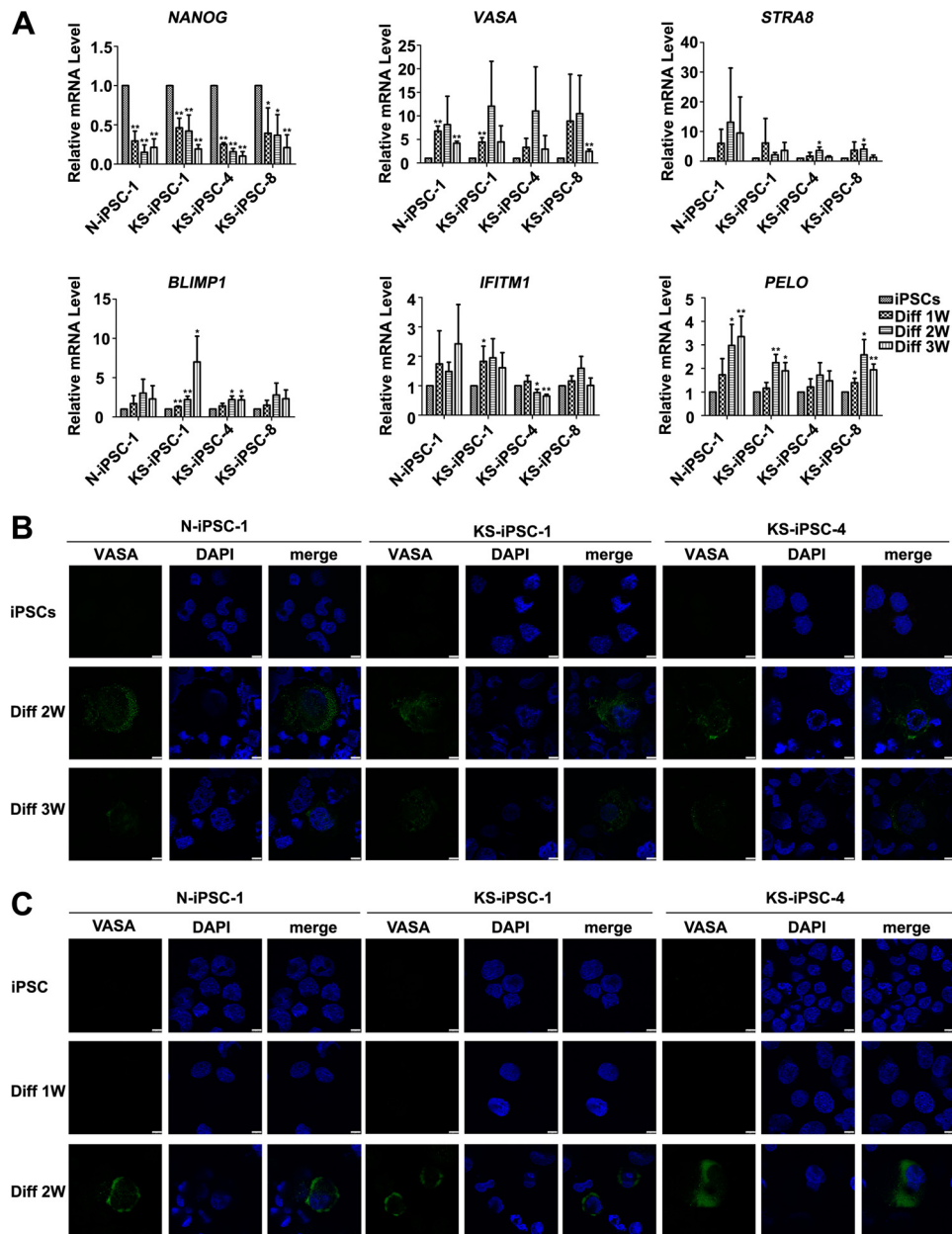


FIGURE 5. Potential of N- and KS-iPSCs to differentiate into germ cell lineages. *A*, quantitative RT-PCR detection of pluripotency-associated marker *NANOG* and the germ cell lineage markers (*VASA*, *STRA8*, *BLIMP1*, *IFITM1*, and *PELO*) during spontaneous differentiation of N-iPSC-1 and KS-iPSC-1, -4, and -8 for 1–3 weeks. Error bars, S.D., *, $p < 0.05$; **, $p < 0.01$, $n = 3$. The expression levels of undifferentiated iPSCs were set as 1. *B*, immunofluorescence staining of *VASA* in differentiated cells of N-iPSC-1 and KS-iPSC-1 and -4 during the spontaneous differentiation for 2 or 3 weeks. Scale bars, 7.5 μm . *C*, immunofluorescence staining examination of *VASA* in N-iPSC-1 and KS-iPSC-1 and -4 during differentiation induced by BMP4, BMP7, and BMP8a for 1 or 2 weeks. Scale bars, 7.5 μm .

sion, and apoptosis (24), being related to the enriched biological process of response to DNA damage stimulus. Also, ZXDA is associated with ZXDC to positively regulate the transcription of the MHC II gene (25), which corresponds to the autoimmune disease pathway and MHC-associated biological processes. Hence, the abnormal expression of these genes may provide the molecular basis for the pathogenesis of KS.

Potentials of iPSCs to Differentiate into Germ Cell Lineages— We next explored the possibility of utilization of KS-iPSCs to either model KS disease development or to generate normal germ cells *in vitro* as a potential treatment for patients. To this end, we differentiated our iPSCs into germ cell lineages. Previ-

ous studies have shown the generation of primordial germ cells and haploid gamete-like cells from hESCs and iPSCs in the early stage of their spontaneous differentiation (26). Consistently, differentiation of N- and KS-iPSCs took place spontaneously after withdrawal of bFGF, as evidenced by the down-regulation of the pluripotency marker Nanog. Simultaneously, expression of germ cell lineage markers was obviously up-regulated without significant difference between N- and KS-iPSCs (Fig. 5*A*). Furthermore, we examined the expression of *VASA* by immunofluorescence staining, which is specially expressed in the germ cell lineage of human beings (27). The differentiated cells expressing *VASA* were detected at 2 and 3 weeks after induc-

tion of differentiation for both N- and KS-iPSCs in a tiny proportion of cells (Fig. 5B). In addition, we also treated iPSCs with BMPs to induce germ cell differentiation, because they were reported to promote hESCs and iPSCs to differentiate into primordial germ cells (28, 29). A small number of VASA-positive primordial germ cell-like cells was found in BMP-treated cells of both N- and KS-iPSCs (Fig. 5C). Thus, our results suggested the potential of KS-iPSCs to differentiate into germ cell lineages.

DISCUSSION

In this study, we generated four lines of KS patient-specific iPSCs and fully characterized them in terms of pluripotency both *in vitro* and *in vivo*, homogeneous XCI after reprogramming, global gene expression profiles, and the potential to differentiate into germ cell lineages. To the best of our knowledge, this is the first study of the XCI, gene expression patterns, and germ cell differentiation potential of iPSCs from the KS patient. The findings obtained here pave the way for our further elucidation of the molecular mechanisms of KS and the development of novel therapies for KS patients.

Female cells carry an X chromosome from each parent, but male cells inherit a single maternal X chromosome. For normal females, the XCI process randomly silences gene expression on one of two X chromosomes early in the development to equalize the dosage of X-linked genes to that of males (22). With respect to KS, a few studies have addressed the issue of XCI in somatic cells of KS patients, favoring the notion that XCI in KS follows the same pattern as in females (30, 31). Here, we report the enrichment of XCI markers (H3K27me3 and macroH2A1) on an inactivated X chromosome (Xi) in all KS iPSCs. By contrast, the proportion of KS fibroblasts with Xi-accumulation of H3K27me3 and macroH2A1 was substantially lower than in KS-iPSCs, being 22% *versus* 100%. Similarly, we also noticed significantly lower Xi accumulation of H3K27me3 and macroH2A1 in normal female fibroblasts than in normal female iPSCs. Currently, we do not know whether the reprogramming process altered the percentage of cells carrying these XCI markers or whether our iPSCs originated from single fibroblasts carrying them. Additionally, it remains elusive whether the fibroblasts without the Xi enrichment of H3K27me3 and macroH2A1 retained an inactive X chromosome or not, as human cells have been shown to display a highly dynamic and variable epigenetic state of the X chromosome (32, 33). Recently, Tchieu *et al.* (20) showed that reprogramming of human somatic cells could return the inactive X chromosome from the maintenance phase to a state resembling the initiation of XCI. The detection of the Xi enrichment of the repressive markers in all KS-iPSCs may also explain their comparable differentiation potential to that of normal iPSCs. Further studies are warranted to define the XCI process in more detail during somatic cell reprogramming in cells with supernumerary X chromosomes.

Nevertheless, the genome-wide comparison of transcriptional profiles of KS-iPSCs with normal 46 XY controls identified significant DEGs, which are over-represented on the X chromosome and known to participate in the biological processes or pathways related to certain clinical features of KS. The

overexpression of X-linked genes could be explained, at least partially, by XCI escaping in KS. However, it remains unclear how the remaining autosomal genes were differentially regulated. One possibility is that the aberrant expression of the autosomal genes was caused by the disturbed expression of X-linked genes. Further exploration of correlations among identified DEGs will answer this question. Previously, Vawter *et al.* (34) found the differential expression of 129 genes by comparing whole genome expression profiles of lymphoblastic cells in KS patients with those in control XY males. They observed dysregulation of X-linked genes and the correlation of 12 genes with measures of verbal cognition in KS patients. There were no overlaps of X-linked DEGs between our work and their data, which may be ascribed to the different cell types tested in these two studies. The DEGs in KS samples identified in our study and other studies will contribute to the elucidation of molecular mechanisms of KS and may serve as biomarkers of KS for early diagnosis or potential therapeutic targets for KS treatment.

It appears that aberrant gene expression in KS-iPSC did not affect their early developmental potential and germ cell lineage commitment as well. The observation is in agreement with the fact that KS patients generally do not display significant symptoms until puberty and hints at the possibility to generate germ cells from KS-iPSCs for the treatment of KS patients suffering from azoospermia. As a matter of fact, mechanisms behind the degeneration of germ cells in KS currently remain unsolved. On the one hand, the supernumerary X itself could prevent the completion of meiosis; on the other hand, an abnormal testicular environment involving somatic Sertoli and Leydig cells could also lead to the failure of generating germ cells. In principle, KS-iPSCs may be induced to differentiate into spermatogonia *in vitro* and then proceed through meiosis. This assumption is supported by studies showing that 47, XXY human cells could lose the supernumerary X chromosome to become 46, XY cells (35). Obviously, more extensive investigations, in particular, cell type-specific differentiation from KS-iPSCs, are needed to find out which cell type(s) is affected by altered gene expression in KS cells. The availability of KS-iPSCs and their utilization in disease modeling will greatly accelerate our understanding, diagnosis, and treatment of Klinefelter syndrome.

REFERENCES

1. Giltay, J. C., and Maiburg, M. C. (2010) Klinefelter syndrome. Clinical and molecular aspects. *Expert Rev. Mol. Diagn.* **10**, 765–776
2. Forti, G., Corona, G., Vignozzi, L., Krausz, C., and Maggi, M. (2010) Klinefelter syndrome. A clinical and therapeutical update. *Sex Dev.* **4**, 249–258
3. Bojesen, A., Birkebæk, N., Kristensen, K., Heickendorff, L., Mosekilde, L., Christiansen, J. S., and Gravholt, C. H. (2011) Bone mineral density in Klinefelter syndrome is reduced and primarily determined by muscle strength and resorptive markers, but not directly by testosterone. *Osteoporos. Int.* **22**, 1441–1450
4. Gravholt, C. H., Jensen, A. S., Høst, C., and Bojesen, A. (2011) Body composition, metabolic syndrome, and type 2 diabetes in Klinefelter syndrome. *Acta Paediatr.* **100**, 871–877
5. Brinton, L. A. (2011) Breast cancer risk among patients with Klinefelter syndrome. *Acta Paediatr.* **100**, 814–818
6. Ross, J. L., Roeltgen, D. P., Stefanatos, G., Benecke, R., Zeger, M. P., Kushner, H., Ramos, P., Elder, F. F., and Zinn, A. R. (2008) Cognitive and motor development during childhood in boys with Klinefelter syndrome. *Am. J.*

- Med. Genet. A* **146**, 708–719
7. Takahashi, K., and Yamanaka, S. (2006) Induction of pluripotent stem cells from mouse embryonic and adult fibroblast cultures by defined factors. *Cell* **126**, 663–676
8. Takahashi, K., Tanabe, K., Ohnuki, M., Narita, M., Ichisaka, T., Tomoda, K., and Yamanaka, S. (2007) Induction of pluripotent stem cells from adult human fibroblasts by defined factors. *Cell* **131**, 861–872
9. Stadtfeld, M., and Hochedlinger, K. (2010) Induced pluripotency: history, mechanisms, and applications. *Genes Dev.* **24**, 2239–2263
10. Grskovic, M., Javaherian, A., Strulovici, B., and Daley, G. Q. (2011) Induced pluripotent stem cells—opportunities for disease modeling and drug discovery. *Nat. Rev. Drug Discov.* **10**, 915–929
11. Li, C., Yu, H., Ma, Y., Shi, G., Jiang, J., Gu, J., Yang, Y., Jin, S., Wei, Z., Jiang, H., Li, J., and Jin, Y. (2009) Germ line-competent mouse-induced pluripotent stem cell lines generated on human fibroblasts without exogenous leukemia inhibitory factor. *PLoS ONE* **4**, e6724
12. Li, C., Zhou, J., Shi, G., Ma, Y., Yang, Y., Gu, J., Yu, H., Jin, S., Wei, Z., Chen, F., and Jin, Y. (2009) Pluripotency can be rapidly and efficiently induced in human amniotic fluid-derived cells. *Hum. Mol. Genet.* **18**, 4340–4349
13. Kitamura, T., Koshino, Y., Shibata, F., Oki, T., Nakajima, H., Nosaka, T., and Kumagai, H. (2003) Retrovirus-mediated gene transfer and expression cloning. Powerful tools in functional genomics. *Exp. Hematol.* **31**, 1007–1014
14. Li, L., Sun, L., Gao, F., Jiang, J., Yang, Y., Li, C., Gu, J., Wei, Z., Yang, A., Lu, R., Ma, Y., Tang, F., Kwon, S. W., Zhao, Y., Li, J., and Jin, Y. (2010) Stk40 links the pluripotency factor Oct4 to the Erk/MAPK pathway and controls extraembryonic endoderm differentiation. *Proc. Natl. Acad. Sci. U.S.A.* **107**, 1402–1407
15. Li, C., Yang, Y., Lu, X., Sun, Y., Gu, J., Feng, Y., and Jin, Y. (2010) Efficient derivation of Chinese human embryonic stem cell lines from frozen embryos. *In Vitro Cell Dev. Biol. Anim.* **46**, 186–191
16. Cheung, A. Y., Horvath, L. M., Grafodatskaya, D., Pasceri, P., Weksberg, R., Hotta, A., Carrel, L., and Ellis, J. (2011) Isolation of MECP2-null Rett syndrome patient hiPS cells and isogenic controls through X-chromosome inactivation. *Hum. Mol. Genet.* **20**, 2103–2115
17. Bucay, N., Yebra, M., Cirulli, V., Afrikanova, I., Kaido, T., Hayek, A., and Montgomery, A. M. (2009) A novel approach for the derivation of putative primordial germ cells and Sertoli cells from human embryonic stem cells. *Stem Cells* **27**, 68–77
18. Lossos, I. S., Czerwinski, D. K., Wechsler, M. A., and Levy, R. (2003) Optimization of quantitative real-time RT-PCR parameters for the study of lymphoid malignancies. *Leukemia* **17**, 789–795
19. Heard, E., and Distech, C. M. (2006) Dosage compensation in mammals. Fine-tuning the expression of the X chromosome. *Genes Dev.* **20**, 1848–1867
20. Tchieu, J., Kuoy, E., Chin, M. H., Trinh, H., Patterson, M., Sherman, S. P., Aimuwu, O., Lindgren, A., Hakimian, S., Zack, J. A., Clark, A. T., Pyle, A. D., Lowry, W. E., and Plath, K. (2010) Female human iPSCs retain an inactive X chromosome. *Cell Stem Cell* **7**, 329–342
21. Tüttelmann, F., and Gromoll, J. (2010) Novel genetic aspects of Klinefelter syndrome. *Mol. Hum. Reprod.* **16**, 386–395
22. Ross, M. T., Grafham, D. V., Coffey, A. J., Scherer, S., McLay, K., Muzny, D., Platzer, M., Howell, G. R., Burrows, C., Bird, C. P., Frankish, A., Lovell, F. L., Howe, K. L., Ashurst, J. L., Fulton, R. S., Sudbrak, R., Wen, G., Jones, M. C., Hurler, M. E., Andrews, T. D., Scott, C. E., Searle, S., Ramser, J., Whittaker, A., Deadman, R., Carter, N. P., Hunt, S. E., Chen, R., Cree, A., Gunaratne, P., Havlak, P., Hodgson, A., Metzker, M. L., Richards, S., Scott, G., Steffen, D., Sodergren, E., Wheeler, D. A., Worley, K. C., Ainscough, R., Ambrose, K. D., Ansari-Lari, M. A., Aradhya, S., Ashwell, R. I., Babbage, A. K., Bagguley, C. L., Ballabio, A., Banerjee, R., Barker, G. E., Barlow, K. F., Barrett, I. P., Bates, K. N., Beare, D. M., Beasley, H., Beasley, O., Beck, A., Bethel, G., Blechschmidt, K., Brady, N., Bray-Allen, S., Bridgeman, A. M., Brown, A. J., Brown, M. J., Bonnin, D., Bruford, E. A., Buhay, C., Burch, P., Burford, D., Burgess, J., Burrill, W., Burton, J., Bye, J. M., Carder, C., Carrel, L., Chako, J., Chapman, J. C., Chavez, D., Chen, E., Chen, G., Chen, Y., Chen, Z., Chinault, C., Ciccocioppa, A., Clark, S. Y., Clarke, G., Clee, C. M., Clegg, S., Clerc-Blankenburg, K., Clifford, K., Cobley, V., Cole, C. G., Conquer, J. S., Corby, N., Connor, R. E., David, R., Davies, J., Davis, C., Davis, J., Delgado, O., Deshazo, D., Dhimi, P., Ding, Y., Dinh, H., Dodsworth, S., Draper, H., Dugan-Rocha, S., Dunham, A., Dunn, M., Durbin, K. J., Dutta, I., Eades, T., Ellwood, M., Emery-Cohen, A., Errington, H., Evans, K. L., Faulkner, L., Francis, F., Frankland, J., Fraser, A. E., Galgoczy, P., Gilbert, J., Gill, R., Glockner, G., Gregory, S. G., Gribble, S., Griffiths, C., Grocock, R., Gu, Y., Gwilliam, R., Hamilton, C., Hart, E. A., Hawes, A., Heath, P. D., Heitmann, K., Hennig, S., Hernandez, J., Hinzmann, B., Ho, S., Hoffs, M., Howden, P. J., Huckle, E. J., Hume, J., Hunt, P. J., Hunt, A. R., Isherwood, J., Jacob, L., Johnson, D., Jones, S., de Jong, P. J., Joseph, S. S., Keenan, S., Kelly, S., Kershaw, J. K., Khan, Z., Kioschis, P., Klages, S., Knights, A. J., Kosiura, A., Kovar-Smith, C., Laird, G. K., Langford, C., Lawlor, S., Leversha, M., Lewis, L., Liu, W., Lloyd, C., Lloyd, D. M., Loulseged, H., Loveland, J. E., Lovell, J. D., Lozano, R., Lu, J., Lyne, R., Ma, J., Maheshwari, M., Matthews, L. H., McDowall, J., McLaren, S., McMurray, A., Meidl, P., Meitinger, T., Milne, S., Miner, G., Mistry, S. L., Morgan, M., Morris, S., Muller, I., Mullikin, J. C., Nguyen, N., Nordsiek, G., Nyakatura, G., O'Dell, C. N., Okwuonu, G., Palmer, S., Pandian, R., Parker, D., Parrish, J., Pasternak, S., Patel, D., Pearce, A. V., Pearson, D. M., Pelan, S. E., Perez, L., Porter, K. M., Ramsey, Y., Reichwald, K., Rhodes, S., Ridler, K. A., Schlessinger, D., Schueler, M. G., Sehra, H. K., Shaw-Smith, C., Shen, H., Sheridan, E. M., Shownkeen, R., Skuce, C. D., Smith, M. L., Sotharan, E. C., Steingruber, H. E., Stewart, C. A., Storey, R., Swann, R. M., Swarbreck, D., Tabor, P. E., Taudien, S., Taylor, T., Teague, B., Thomas, K., Thorpe, A., Timms, K., Tracey, A., Trevanion, S., Tromans, A. C., d'Urso, M., Verdusco, D., Vilasana, D., Waldron, L., Wall, M., Wang, Q., Warren, J., Warry, G. L., Wei, X., West, A., Whitehead, S. L., Whiteley, M. N., Wilkinson, J. E., Willey, D. L., Williams, G., Williams, L., Williamson, A., Williamson, H., Wilming, L., Woodmansey, R. L., Wray, P. W., Yen, J., Zhang, J., Zhou, J., Zoghbi, H., Zorilla, S., Buck, D., Reinhardt, R., Poustka, A., Rosenthal, A., Lehrach, H., Meindl, A., Minx, P. J., Hillier, L. W., Willard, H. F., Wilson, R. K., Waterston, R. H., Rice, C. M., Vaudin, M., Coulson, A., Nelson, D. L., Weinstock, G., Sulston, J. E., Durbin, R., Hubbard, T., Gibbs, R. A., Beck, S., Rogers, J., and Bentley, D. R. (2005) The DNA sequence of the human X chromosome. *Nature* **434**, 325–337
23. Scofield, R. H., Bruner, G. R., Namjou, B., Kimberly, R. P., Ramsey-Goldman, R., Petri, M., Reveille, J. D., Alarcón, G. S., Vilá, L. M., Reid, J., Harris, B., Li, S., Kelly, J. A., and Harley, J. B. (2008) Klinefelter syndrome (47,XXY) in male systemic lupus erythematosus patients. Support for the notion of a gene-dose effect from the X chromosome. *Arthritis Rheum.* **58**, 2511–2517
24. Barker, P. A., and Salehi, A. (2002) The MAGE proteins. Emerging roles in cell cycle progression, apoptosis, and neurogenetic disease. *J. Neurosci. Res.* **67**, 705–712
25. Al-Kandari, W., Koneni, R., Navalgund, V., Aleksandrova, A., Jambunathan, S., and Fontes, J. D. (2007) The zinc finger proteins ZXDA and ZXDC form a complex that binds CIITA and regulates MHC II gene transcription. *J. Mol. Biol.* **369**, 1175–1187
26. Eguizabal, C., Montserrat, N., Vassena, R., Barragan, M., Garreta, E., Garcia-Quevedo, L., Vidal, F., Giorgetti, A., Veiga, A., and Izpisua Belmonte, J. C. (2011) Complete meiosis from human-induced pluripotent stem cells. *Stem Cells* **29**, 1186–1195
27. Castrillon, D. H., Quade, B. J., Wang, T. Y., Quigley, C., and Crum, C. P. (2000) The human VASA gene is specifically expressed in the germ cell lineage. *Proc. Natl. Acad. Sci. U.S.A.* **97**, 9585–9590
28. Kee, K., Angeles, V. T., Flores, M., Nguyen, H. N., and Reijo Pera, R. A. (2009) Human DAZL, DAZ, and BOULE genes modulate primordial germ-cell and haploid gamete formation. *Nature* **462**, 222–225
29. Panula, S., Medrano, J. V., Kee, K., Bergström, R., Nguyen, H. N., Byers, B., Wilson, K. D., Wu, J. C., Simon, C., Hovatta, O., and Reijo Pera, R. A. (2011) Human germ cell differentiation from fetal- and adult-derived induced pluripotent stem cells. *Hum. Mol. Genet.* **20**, 752–762
30. Iitsuka, Y., Bock, A., Nguyen, D. D., Samango-Sprouse, C. A., Simpson, J. L., and Bischoff, F. Z. (2001) Evidence of skewed X-chromosome inactivation in 47,XXY and 48,XXYY Klinefelter patients. *Am. J. Med. Genet.* **98**, 25–31
31. Poplinski, A., Wieacker, P., Kliesch, S., and Gromoll, J. (2010) Severe XIST hypomethylation clearly distinguishes (SRY+) 46,XX-male from Klinefelter syndrome. *Eur. J. Endocrinol.* **162**, 169–175

- 32. Hoffman, L. M., and Carpenter, M. K. (2005) Characterization and culture of human embryonic stem cells. *Nat. Biotechnol.* **23**, 699–708
- 33. Silva, S. S., Rowntree, R. K., Mekhoubad, S., and Lee, J. T. (2008) X-chromosome inactivation and epigenetic fluidity in human embryonic stem cells. *Proc. Natl. Acad. Sci. U.S.A.* **105**, 4820–4825
- 34. Vawter, M. P., Harvey, P. D., and DeLisi, L. E. (2007) Dysregulation of X-linked gene expression in Klinefelter syndrome and association with verbal cognition. *Am. J. Med. Genet. B Neuropsychiatr. Genet.* **144B**, 728–734
- 35. Kawakami, T., Zhang, C., Taniguchi, T., Kim, C. J., Okada, Y., Sugihara, H., Hattori, T., Reeve, A. E., Ogawa, O., and Okamoto, K. (2004) Characterization of loss-of-inactive X in Klinefelter syndrome and female-derived cancer cells. *Oncogene* **23**, 6163–6169